Chapter 11
Spontaneous Structuration of Hydrophobic Polymer Surfaces in Contact with Salt Solutions

Igor Siretanu, Hassan Saadaoui, Jean-Paul Chapel, and Carlos Drummond

It has been described in previous chapters how spontaneous instabilities related to interfacial phenomena can be used to produce controlled patterns on polymer surfaces. Strategies of polymer patterning assisted by dewetting or water drop condensation were described. In this chapter we present a waterborne process based on the interaction between ions in water and hydrophobic polymer surfaces, modulated by the gases dissolved in the aqueous phase. We show how by controlling this interaction the polymer surface can be conveniently modified. In the first section of the chapter we describe some aspects of the interface between water and a hydrophobic surface. We then describe how the composition of the aqueous phase can have important consequences on the morphology of the hydrophobic surface, and then illustrate how this process can be conveniently used to modify the morphology of a hydrophobic polymer in a controlled manner.

11.1 Water-Hydrophobic Interfaces, WHI: A Deceptively Simple System

The interface between water and hydrophobic surfaces plays a central role in a number of important subjects. Proteins folding, self-assembly, detergency, or oil recovery are just few examples of important problems involving the contact between water and a hydrophobic surface. Nevertheless, a complete description

I. Siretanu (✉)
Physics of Complex Fluids, MESA Institute for Nanotechnology, University of Twente, Post Office Box 217, 7500 AE Enschede, The Netherlands
e-mail: i.siretanu@utwente.nl

H. Saadaoui • J.-P. Chapel • C. Drummond
CNRS, Centre de Recherche Paul Pascal (CRPP), UPR 8641, 33600 Pessac, France

Centre de Recherche Paul Pascal, Université de Bordeaux, 33600 Pessac, France

J. Rodríguez-Hernández, C. Drummond (eds.), *Polymer Surfaces in Motion*,
DOI 10.1007/978-3-319-17431-0_11

of WHI is yet to be reached. In particular, two aspects related to the process discussed in this chapter have been the subject of some controversy: the presence of a layer of reduced water density near the WHI and the adsorption of ions on them.

When water is in contact with air in standard conditions, oxygen and nitrogen are dissolved in concentrations of 0.2 mM and 0.5 mM, respectively. There is a general consensus that when a hydrophobic surface is in contact with water, the fluid density is substantially reduced in the vicinity of the surface. On the contrary, the reasons behind this depleted layer and its actual structure are still subjects of debate. It has been reported that dissolved gases can adsorb on hydrophobic surfaces in the form of small spherical caps (nanobubbles) [1] or flattened objects [2, 3] (micropancakes; it has been argued that these are just bubbles with a large but well-defined radius of curvature in order to satisfy Laplace's equation [4]) or as a reduced-density continuous interfacial layer. After they were first proposed about 20 years ago [1], many experimental studies have reported the existence of nanobubbles on hydrophobic surfaces. In most of them, tapping-mode atomic force microscope has been used to image the bubbles under gentle perturbation [5]. An example of nanobubble formation on a hydrophobic surface is presented in Fig. 11.1a. It has been suggested that the high-frequency oscillatory motion of the AFM tip may be responsible for nanobubble nucleation. However, other techniques (infrared spectroscopy [6], surface plasmon resonance [7], optical interference-enhanced reflection microscopy [8], and rapid cryofixation/freeze fracture [9]) have reinforced the idea of their existence.

The mere existence of gaseous nanostructures (GNs) on surfaces has been the subject of scorching debates in the literature. This is partially due to the fact that their materialization and stability appear to be extremely sensitive to the experimental conditions, as was recently shown by Seddon and coworkers [10]. However, the existence of GN on hydrophobic surfaces is gaining consensus in the scientific

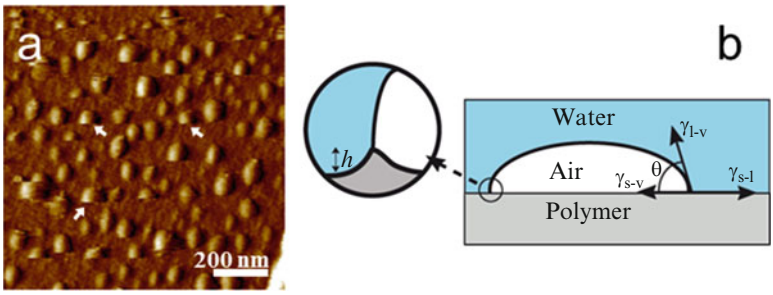

Fig. 11.1 (**a**) Contact-mode AFM deflection images of PS in water. The presence of nanobubbles is observed. Occasionally the bubbles are removed by the effect of the tip; only a portion of the nanobubble appears in the image (*white arrows*). (**b**) Schematic representation of a nanobubble in a water/polymer interface. The contact angle θ is determined by the equilibrium between the horizontal forces in the triple solid–liquid–vapor contact line: liquid–vapor $\gamma_{l\text{-}v}$, solid–liquid $\gamma_{s\text{-}l}$, and solid–vapor $\gamma_{s\text{-}v}$ interfacial tensions. The vertical component of the liquid–vapor interfacial tension, $\gamma_{l\text{-}v}\sin(\theta)$, is equilibrated by a deformation of the substrate, as described in the text

community, after a large number of papers have been published in that subject. On the contrary, the reasons for their stability remain unclear. It has often been argued that because of their small radii of curvature, the excess Laplace pressure inside the nanobubbles ($\Delta P = 2\gamma/R$, where γ is the water-air interfacial tension and R the GN radius of curvature) should lead to their immediate disappearance: the bubbles are diffusively unstable. Even though R of the GN is larger than it may appear from their typical nanometric size height (because of the unusually low contact angle of the GN on hydrophobic surfaces), the excess Laplace pressure inside the GN is of the order of few atmospheres, which leads to estimations of lifetimes of the order of microseconds [5]. Nevertheless, it has been repeatedly observed that adsorbed nanobubbles can be stable for as long as few days, suggesting that they are thermodynamically stable.

Several theories have been advanced to explain this anomaly. Spurious contamination has been evoked several times. As everybody recognizes, it is extremely difficult to keep water and hydrophobic surfaces contamination free. Minute amounts of surface-active contaminants could be responsible for the unexpected stability of the GN [11]. However, the widespread presence of GN hints for more fundamental reasons behind their stability. Dynamic stationary models based on continuous gas flow between the bubbles and the surroundings have also been proposed [12]. However it is unclear what would be the driving force for the continuous gas flow. As some ions naturally adsorb on hydrophobic surfaces in contact with water, models based on the pressure due to the presence of charges adsorbed at the interface have also been discussed [13]. Attard recently proposed that gas supersaturation on the aqueous phase can explain both the stability and the anomalous contact angle, due to reduction in the water vapor interfacial tension [4]. This model conciliates the existence of the GN with Laplace's equation. However, it imposes supersaturation as a *sine qua non* condition for the existence of GN, which has been contested by other groups [10]. In addition, it is not clear why a long-lasting vapor supersaturation is observed in many different experimental situations. In summary, the reasons for the stability of GN are yet to be soundly established; for our purposes, it suffices to recognize their existence and stability. As discussed in next chapter and mentioned in next section, this may have important implications in the morphology of polymer surfaces in contact with water.

Another puzzling aspect of WHI is the fact that they are often electrically charged. In the absence of dissociating groups, this can only be due to ion adsorption, even though ions should strongly partition into the aqueous phase of higher dielectric constant [14]. Different mechanisms—entropy changes [15], ionic asymmetry [16], ionic polarizability [17], and ionic induced decrement of water polarization fluctuations [18, 19]—have been evoked to explain this fact. A satisfactory description of a charged interface at low-salt concentrations can be achieved by mean field theories, developed after the work of Gouy and Chapman, which is the starting point for the celebrated Poisson-Boltzmann equation [20]. One aspect that cannot be accounted for by this simple description is the distinct effect of particular ions, because it only considers the ionic charge, and does not take into account the discrete nature of ions or solvent molecules, or the possibility of correlation

between the charges. The error introduced by considering ions as indistinct point charges, neglecting the dispersion forces involving the ions and their disruptive effect on the solvent, becomes unacceptable as ionic strength increases. Another source of error that is frequently overlooked is related to the deformability of the boundary: the walls are often considered to be unalterable and non-deformable. This assumption is adequate for hard solid walls, but is certainly not so for soft boundaries, e.g., charged membranes or polymer substrates. In this sense, we have observed that smooth, hydrophobic polymer surfaces can be substantially deformed due to the effect of adsorbing ions. We have called this phenomenon ion-induced polymer nanostructuration, IPN [21]. We describe the IPN process in detail in the rest of this chapter. Some examples of how this method can be used to control the morphology of polymer surfaces are advanced in the last section.

11.2 Ionic Solutions in Contact with Hydrophobic Polymers: Ion-Induced Polymer Nanostructuration

We discuss now how the morphology of a hydrophobic polymer can be modified by the contact with water. For the reasons described in previous section, this transformation depends on the amount of gases dissolved and the ionic species present. The typical size and nature of formed pattern can then be tuned if these variables are precisely controlled. Two processes must be considered. First, the GNs have a transforming effect, as described in next chapter. Second, the specific adsorption of ions may induce spontaneous surface deformation.

Reducing the concentration of the gases dissolved in water may deeply affect many interfacial properties. Despite the fact that oil and water do not mix, spontaneous emulsification of hydrocarbons occurs after water degassing [22–24]. Colloid stability [25], the range of the hydrophobic interaction [26], the conductivity of salt solutions [27], the efficiency of flotation process [28], and the slippage boundary conditions in flowing water [29] are all affected by the amount of gas in solution. The amount of gas dissolved has also significant consequences on the morphology of a surface in contact with the aqueous phase. Several workers have shown how the presence of GNs can induce surface modification. Wang and coworkers [30] reported the formation of nanoindents in very thin films of polystyrene (<5 nm) (PS) after few tens of minutes of exposure to water. Similar results were reported by Mazumder and Bhushan [13] after exposing PS films (25 nm thick) to deionized water. Janda and coworkers [31] reported the exfoliation and indentation of highly ordered pyrolytic graphite in contact with nanobubbles. Tarábková and Janda [32] reported a netlike nanopatterning of thin PS films (around 10 nm) in contact with nanobubbles. A complete description of this subject is discussed in next chapter.

Even in the absence of dissolved gas, polymer surfaces may be modified in contact with water. As advanced above, we have observed that the adsorption of specific ions on hydrophobic polymers can induce important surface

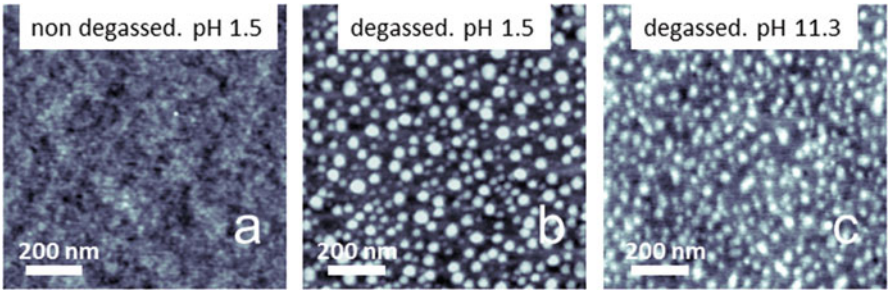

Fig. 11.2 1 μm × 1 μm height tapping-mode AFM micrographs taken in air of 300 nm thick 250 kDa polystyrene films after exposure to a non-degassed (**a**) and degassed solution of nitric acid at pH 1.5 (**b**) and sodium hydroxide at pH 11.3 (**c**) in double-distilled water and room temperature. The presence of asperities of regular nanometric size is observed on the surface exposed to the degassed solutions for 5 min. On the contrary, no modification was detected when an identical film was exposed to the same solution under identical conditions (or much longer times) before removing the dissolved gases. XPS tests showed that no chemical modification of the films has occurred

transformations. For this to happen, the intimate contact between the aqueous phase and the polymer has to be favored by the removal of gases dissolved in the water. Water degassing avoids formation of GNs, allowing the direct adsorption of ions to the interface. As an example, when polystyrene films are put in contact with degassed water solutions of acidic or basic pH for a few minutes, a long-lasting nanostructuration spontaneously forms on the solid surface, as illustrated in Fig. 11.2. This only happens in the presence of certain ions; otherwise no modification of the polymer film is observed. The typical size of the self-assembled patterns depends on pH, type, and concentration of dissolved salts; temperature and amount of dissolved gas in the aqueous phase; as well as mobility of the surface, which can be affected by the interaction with the supporting substrate.

The examples shown in Fig. 11.2 correspond to thin films of polystyrene in contact with acidic or basic water. The surface structuration has no effect on the wettability of the surfaces: the contact angle of water on the substrate is not changed by the process. The morphology change is not accompanied by any chemical modification. However, the hydrophobicity of the surface seems to determine the outcome of the process: the structuration of the film is not observed if the polymer surface is rendered hydrophilic ($\theta = 30°$) before the water treatment by partial UV oxidation. Two remarkable conclusions can be drawn from this interesting effect. First, the interaction between the aqueous phase and the hydrophobic substrate is fundamentally modified by the gases dissolved which shelter the hydrophobic substrate from the aqueous phase. Second, there is a mobile surface layer on the polymer which can be restructured under external stimuli, even though we are working at temperatures largely below the glass transition temperature T_g of PS. This indicates that macromolecular chains near the interface have properties which deviate significantly from their bulk counterparts. Indeed, no structuration

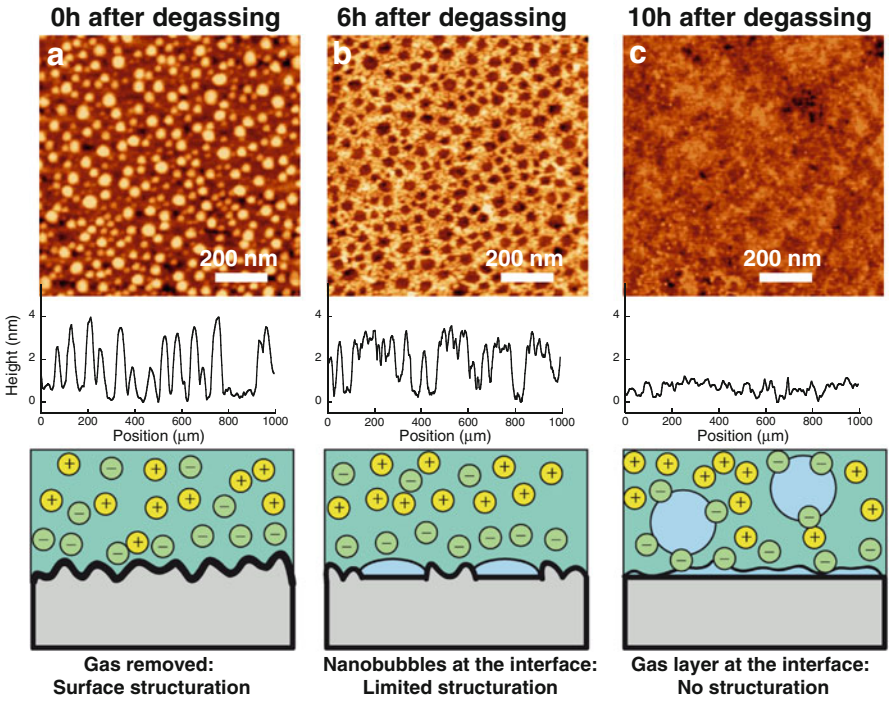

Fig. 11.3 The amount of dissolved gas determines the nature and extent of the surface structuration. 300 nm thick 250 kDa PS films were immersed during 10 min in water at pH 1.5 and then studied by AFM in air. Before treating the surfaces, the aqueous solution was in contact with air during different periods of time after degassing as indicated, to change the amount of gas dissolved. (**a**) Shortly after degassing the preferential adsorption of ions at the water/polymer interface is likely to be responsible for the observed self-assembled nanostructure. Increasing amounts of gas in the solution move the ions away from the polymer surface limiting the structuration below the bubbles (**b**), or the low-density layer (**c**). Adapted with permission from [21]. Copyright (2011) American Chemical Society

was observed in films of UV cross-linkable PS after UV curing, evidencing the importance of surface mobility.

It is very revealing to explore the effect of the amount of gas dissolved on IPN. As can be observed in Fig. 11.3, the size of the observed bumps is larger at short times after degassing. Ten hours after degassing water has regained its equilibrium with the atmosphere, no structuring effect is detected. On the contrary, at intermediate times a seemingly different structuration effect is observed: the contact with the aqueous phase induces the formation of a regular array of shallow holes/rims (nanoindents) in the polymer film, with a typical size of 30 nm and depth of 2 nm. The thickness of the structured region (between 2 and 3 nm) is consistent with recent reports of the presence of a thin mobile layer on the surface of glassy PS films [33].

Our understanding of the fundamental reasons behind these phenomena is far from being complete. Some preliminary and speculative ideas waiting to be

validated are described here. At low concentration of dissolved gas (cf. Fig. 11.3a), the preferential adsorption of ions at the interface induces the formation of bumps. As mentioned above, it has long being recognized that pristine water/oil interfaces can become charged due to adsorption of ions. It is only in the presence of adsorbing ions that IPN is observed: we believe that the observed surface structuration is related to the electric field originated by their presence. As mentioned above, the discontinuity in dielectric constant conspires against ion adsorption on the interface [14]. However, if other forces promote ion adsorption (e.g., ion-dispersion forces [34], "cavity" forces, due to perturbation of the hydrogen bond network of water [35]), subsequent reconstruction of the interface, driven by electrostatic, can then arise to reduce the total energy of the system. Some examples related to this phenomena can be found in the literature; membrane deformation by interaction with ions was discussed few decades ago by Parsegian [36]; water-air interfacial deformation in the presence of adsorbing ions has been predicted by molecular dynamic simulations [37]. The complete description of this problem requires integrating the viscoelastic and plastic properties of the polymer film. In addition, the film shape and the electrostatic boundary conditions are intermingled and cannot be treated independently: the presence of the ions distorts the shape of the surface, changing the boundary conditions of the electrostatic problem that determines the ionic distribution.

At large gas concentration larger bubbles or even a continuous low-density layer is present at the water/polymer interface and no structuration effect is detected (Fig. 11.3c). Finally, at intermediate gas concentrations a layer of nanobubbles nucleate on the surface, which is responsible for the netlike pattern observed (Fig. 11.3b). The formation of a similar pattern has been reported by Wang and coworkers [30], and is certainly related to the process of nanobubble-assisted nanostructuration described in next chapter. They suggested that the combination of increased Laplace pressure and interfacial tension is at the origin of the nanoindents observed. The problem of the elastic deformation of soft surfaces due to the vertical component of the interfacial tension when a liquid drop (or a gas bubble) is posed in the surface has been discussed in the literature. The surface modification shown in Fig. 11.3 is long lasting, indicating an irreversible (plastic) deformation. However, we can try to estimate the order of magnitude of the deformation ridge h using the elastic model described by Shanahan and Carré [38]. By equating the vertical component of the interfacial tension to the elastic stress field on the solid surface, one obtains $h \approx \gamma_{LV} \cdot \sin\theta/G$, where G is the shear modulus of the solid and γ_{LV} the water-air interfacial tension (cf. Fig. 11.1b). If G and θ for bulk polystyrene and γ_{LV} for air-water are considered, h values of the order of 10^{-12} m are obtained, much smaller than the deformation observed experimentally. The inconsistency is even more important if experimental values of the contact angle θ typically observed for nanobubbles are considered. Several reasons could be evoked to account for this discrepancy. The value of G of the polymer surface is probably smaller than the bulk value. Recently, by studying the relaxation of nanometric deformations on films of PS, Fakhraai and Forrest showed that the mobility of polymer chains is dramatically accelerated nearby the surfaces

with respect to the bulk [33]. Although it is still poorly understood, several explanations have been advanced for this enhanced dynamic, related to the reduced entanglement density, enrichment of chain ends, and increased free volume for the polymer molecules at the surface. Another possible explanation is that water may have a plasticizing effect on the polymer effectively reducing G. However, it is difficult to conceive a reduction of G of three orders of magnitude, which is necessary to account for the discrepancy observed. The effect of adsorbing ions may also be important. As can be observed in the AFM micrographs, small bumps are still formed in the region between or at the rim of the nanobubbles. Hence, the observed deformation at intermediate concentrations may be related to the transforming effect of the adsorbing ions, as in the case of complete degassing, as illustrated in Fig. 11.3.

For the rest of this chapter we describe the IPN process: the influence of some variables that determine the outcome of the process and how it can be used to achieve easy polymer patterning in a single step.

11.3 IPN: Ionic Specificity

We found that the IPN process is ion specific: in the absence of adsorbing ions in the aqueous phase no structuring effect was observed. Some examples of structuring and non-structuring ions are presented in Fig. 11.4. In all cases, the IPN was correlated with ion adsorption, which was indirectly determined by measuring the electrokinetic zeta potential of PS films in contact with salt solutions. From our studies, several general trends were recognized:

- Substantial PS structuration is observed in the presence of water ions ($pH < 2.5$ or $pH > 10$). The deformation of the hydrophobic polymer surface at different pH values indicates a greater influence of the presence of hydroxide ions compared with protons: for example, similar surface patterning is obtained at pH 1.5 and 11, even though the $[H_3O^+]$ in the former case is much larger than the $[OH^-]$ in the latter. This result suggests a preferential adsorption of OH^- with respect to H_3O^+ on the hydrophobic substrate. It has been reported many times that hydrophobic interfaces and even gas bubbles are negatively charged in contact with water at neutral or basic pH and become positively charged in acidic solutions [39]. The origin of this charge is hotly debated. The main disagreement comes from the fact that the majority of experiments suggest a preferential adsorption of hydroxide ions [39], while the opposite picture has emerged from reports of surface-sensitive spectroscopic techniques and MD simulations [40]. Our results point in the direction of preferential OH^- adsorption.
- Degassed solutions of most inorganic electrolytes evaluated did not induce large structuration on PS surfaces. Some examples are presented in Fig. 11.4. With this kind of salts, the observed mild surface deformation is similar to the one

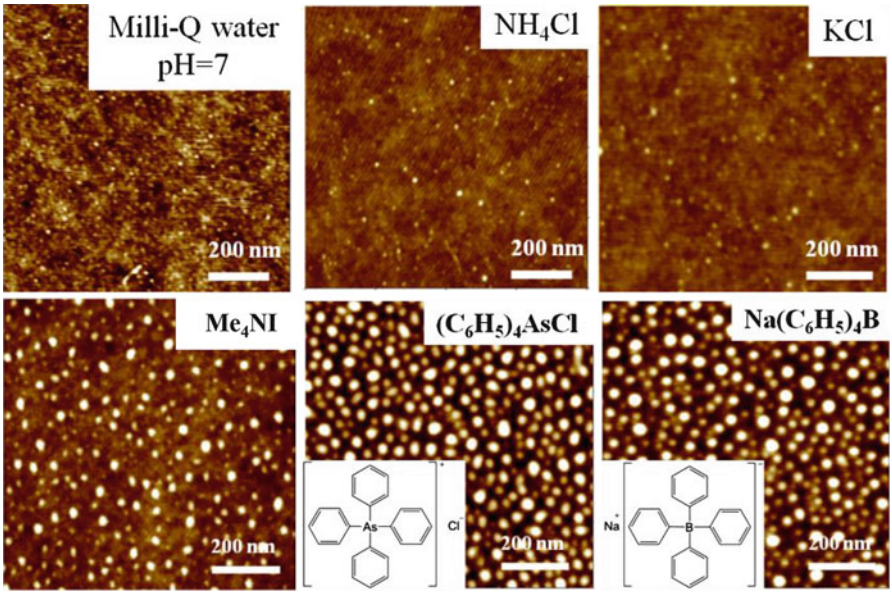

Fig. 11.4 AFM micrographs of 300 nm thick PS films after 5-min exposure to water or 0.03 M degassed aqueous solutions of ammonium chloride, potassium chloride, tetramethyl ammonium iodide, tetraphenyl arsonium chloride, Ph_4AsCl, and sodium tetraphenylborate, $NaPh_4B$

obtained by treatment with degassed water at neutral pH. As a remarkable exception to this rule, relatively large bumps (although at a lesser density) are observed after treatment of PS surfaces with degassed solutions of some lithium salts (see below).

– Degassed aqueous solutions of amphiphilic ions (e.g., sodium dodecyl sulfate, SDS, dodecyl trimethyl ammonium bromide, DTAB) or hydrophobic ions (e.g., halides of tetra-alkyl-ammonium quaternary, Ph_4BNa or Ph_4AsCl) induce substantial deformation of the PS surfaces. The hydrophobicity of the ion seems to have a distinctive influence on the nanostructuration. The longer is the chain length of tetra-alkyl-ammonium iodide salts the larger is the typical size of the induced nanostructure. Furthermore, ions with similar molecular structure seem to induce similar nanostructuration effect, regardless of the sign of the charge. For example, the salt Ph_4BNa induces the same effect as Ph_4AsCl (Fig. 11.4), probably due to the similar effect of the tetraphenyl ions of opposite charge.
– The observed nanostructuration is not just due to the effect of a particular ion, but to the combined influence of the different ions present in solution. For example, the structuration effect of tetrabutylammonium salts is different for different counterions. The size of the bumps was larger for the case of iodide or bromide compared with nitrate or chloride. A more marked difference is observed for the case of lithium salts. While LiCl and $LiSO_4$ did not induce extensive surface structuration, substantial effect of LiI and LiBr solutions was

observed. As a comparison, sodium or potassium salts with similar counterions did not produce any noticeable surface modification.

– For salts that do not provoke extensive structuration of PS surfaces, there is no appreciable effect of salt concentration up to 0.1 M. This indicates that the small structuration observed in these cases is mainly determined by the small amount of water ions present in the solutions. On the contrary, for salts with larger structuring influence, the resulting morphology depends on salt concentration. In general, higher concentrations result in higher surface charge density and in a more important modification of the polymer surface. Typically, the surface structuration was no longer enhanced for concentrations above 0.03 M.

An extensive report on ionic specificity in IPN was recently published [41].

11.4 Thermal Effects in IPN

As can be observed in Fig. 11.5, the typical size of the self-assembled pattern is strongly modified by the temperature during treatment. We can distinguish two different scenarios. At low temperature ($T < 30$ °C) a monomodal bump size

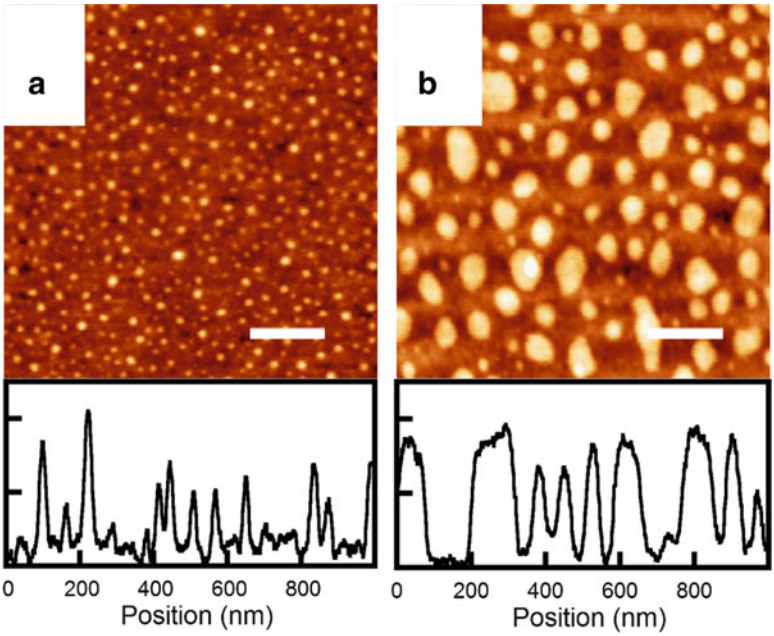

Fig. 11.5 1 μm × 1 μm height tapping-mode AFM micrographs taken in air of 300 nm thick 250 kDa PS films after exposure to degassed solutions of nitric acid in double-distilled water at pH 1.5. The temperature during treatment was (**a**) 25 °C and (**b**) 70 °C. A typical height profile for each condition is presented. The presence of self-assembled asperities (*bumps*) is observed only on the surfaces exposed to the degassed solution for 1 min. The scale bars correspond to 200 nm

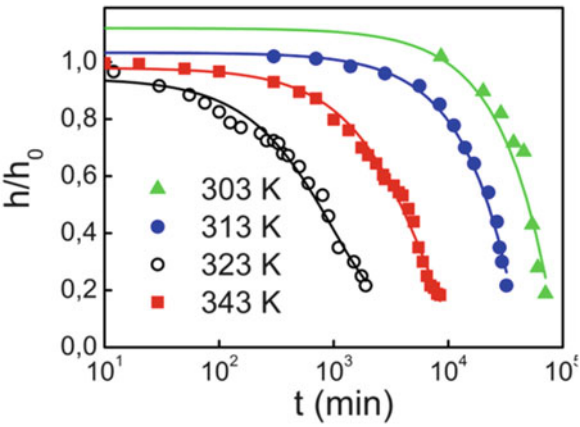

Fig. 11.6 Temporal evolution of the bump height for surfaces nanostructured at 25 °C aged at different temperatures. The continuous lines correspond to least-squares fits to exponential decay of the data at times longer than the decay time

distribution is observed. On the contrary, the size distribution increasingly broadens as the temperature of treatment is increased. The broad distribution is observed right after the treatment; it is not a consequence of the temporal evolution of the polymer surface. As can be observed in Fig. 11.5, the areal fraction occupied by large bumps increases with temperature of treatment, occupying most of the surface at 70 °C; however, zones of small bumps ($r < 30$ nm) can always be identified.

The subsequent evolution of the self-assembled structure is determined by the environmental conditions. The structure disappears after the structured surface is annealed at 95 °C for a few hours. Nevertheless, these patterns reappear if the surface is exposed again to degassed aqueous solutions. The patterns also relax under solvent annealing: after exposure to toluene vapor for 1 h most of the structuration is removed. Indeed, the surface of the film slowly relaxes back to the original smooth condition even when the films are conserved in air at room temperature. We observed a faster evolution of the films of PS of lower molecular weights. The temporal evolution for mean bump height at different temperatures below T_g is presented in Fig. 11.6a. For a number of samples structured under identical conditions at 25 °C, as can be expected, the relaxation time markedly decreases with increasing temperature. The relaxation process can be used to study the viscoelastic properties of the polymer surface, as has been described in studies of relaxation of grating-shaped surfaces [42] or nanoholes [33]. In agreement with these earlier studies, a significant reduction in T_g near the film surface is supported by our results.

11.5 IPN: Remote Control of Surface Structuration

IPN is due to partial reconstruction of the polymer surface. It is interesting to explore how deep in the film the surface modification is propagated. We have observed that the IPN surface pattern can be altered by modifying the substrate

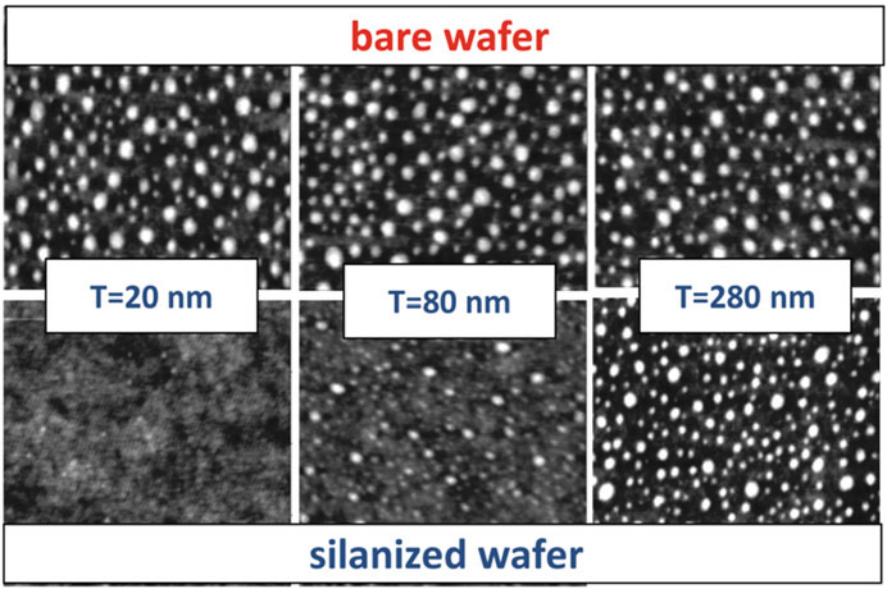

Fig. 11.7 Height AFM micrographs of films of 250 kDa polystyrene films measured in tapping mode in air. The films of indicated thickness were spun coated on bare and silanized silicon wafers (fractional OTS surface coverage 0.7) and then exposed to a degassed solution of nitric acid in double-distilled water at pH 1.5 at room temperature. The presence of asperities of regular nanometric size is clearly observed on some of the films exposed to the degassed solution during 5 min. The silanization of the wafer blocked the structuration of films thinner than the end-to-end radius of the polymer. All the films were featureless before treatment

supporting the film, as shown in Fig. 11.7. The typical radii and heights of the bumps formed in the surface are similar in oxidized Si wafers, and are independent of polymer film thickness down to 10 nm. On the contrary, the characteristic size of the bumps is substantially reduced—or they are not present—for films deposited on hydrophobized wafers for polymer films thinner than the end-to-end radius of the polymer. As mentioned above, the idea that polymer segments close to the surface are more mobile than bulk segments is now broadly accepted, although the properties of the mobile layer (thickness, variation with temperature, and molecular weight) are still debated. On the contrary, it is not obvious why this excess mobility should be impaired by the influence of the underlying substrate buried down several tens of nanometers below the polymer film surface.

The threshold thickness for surface structuration is determined by polymer size: the larger the molecular weight, the longer the range of the effect of the substrate on the structuration of the polymer layer. In all cases the observed effect has a range too large—up to 100 nm for the largest polymer investigated—to be interpreted in terms of the dispersion interaction between the solid substrate and water through the polymer film. The reason for the long-range effect of the substrate on the polymer structuration is related to the connectivity of the polymer chains. A complete study of this effect has been reported before [43].

11.6 IPN: An Easy Waterborne Process for Polymer Surface Structuration

The procedure described here may be of interest for producing controlled nanostructured structures on flat, non-planar, or hollow hydrophobic substrates in a single simple step allowing an easy and precise control of the nanopatterns produced. Some realizations of this idea are presented in Fig. 11.8: the nanostructuration of a monolayer of PS microspheres—a substrate that would be impossible to pattern with conventional lithographic techniques—or the selective patterning of a PS substrate partially protected by a PDMS mask were performed in a simple waterborne step. Selective patterning of the surface of a polymer film can be achieved if the film is deposited on a patterned substrate that selectively avoids IPN to proceed, taking advantage of the process described in the previous section, as illustrated in Fig. 11.9.

The obtained patterned polymer surfaces can also be replicated by metal thermal evaporation to produce nanostructured metallic films with holes or asperities of controlled size, as illustrated in Fig. 11.10. After deposition of a sufficiently thick metal layer, the polymer layer can be cleaved or dissolved away. This procedure allows an efficient and precise control of the metallic surface structure, with possible applications in materials science and photonics. The roughness of polydimethylsiloxane (PDMS) surfaces can be tuned by this technique if the PDMS is treated while cross-linking, which may be of interest for microfluidic applications. We have also observed that substrates of poly(methyl methacrylate) (PMMA), PS in the form of colloidal spheres and bulk, and semicrystalline films of polyethylene (PE) are prone to be structured by this technique, evidencing the versatility and potential for its widespread use. It may find applications in many different scientific and technological fields like nanolithography, microfluidics, or flexible electronics.

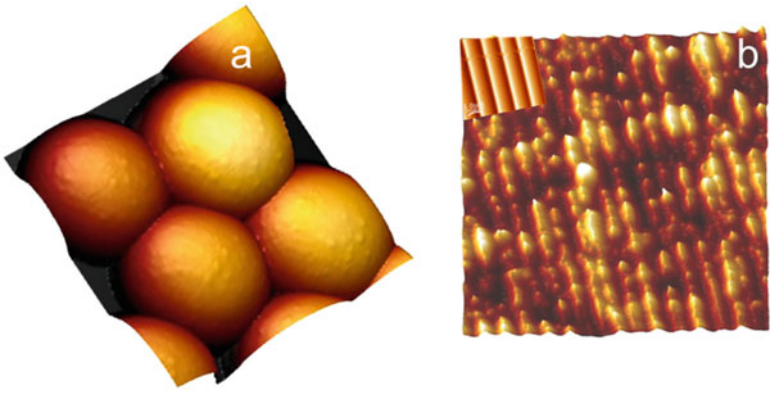

Fig. 11.8 AFM micrographs taken in air show that the surface nanostructuration was also observed in (**a**) a layer of PS latex (radii 0.2 μm) deposited by dip-coating from a concentrated aqueous solution (10 g/l) on top of a smooth mica surface, (**b**) in bulk PS partially protected by a sinusoidal micro-wrinkled PDMS stamp ($\lambda = 2$ μm; see *inset*). Adapted with permission from [21]. Copyright (2011) American Chemical Society

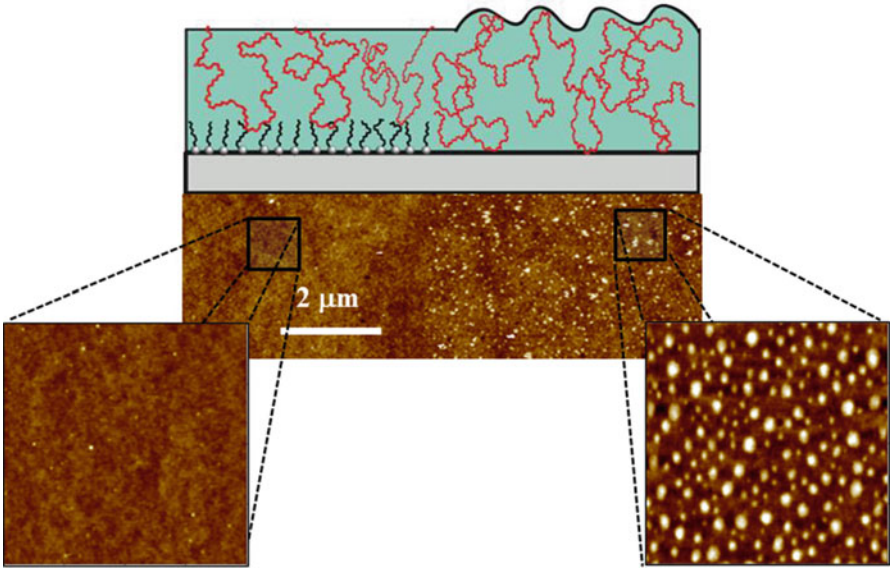

Fig. 11.9 Height tapping-mode AFM micrograph measured in air of 50 nm thick 250 kDa polystyrene films after exposure to a degassed solution of nitric acid in double-distilled water during 5 min. pH 1.5; T 25 °C. The film was spin coated on a half silanized silicon wafer. Scale bar corresponds to 2 µm. The presence of asperities of regular nanometric size bumps is clearly observed on the bare silicon wafer. On the contrary, no modification was detected in the region which was coated with OTS. Adapted with permission from (47). Copyright (2011) American Chemical Society

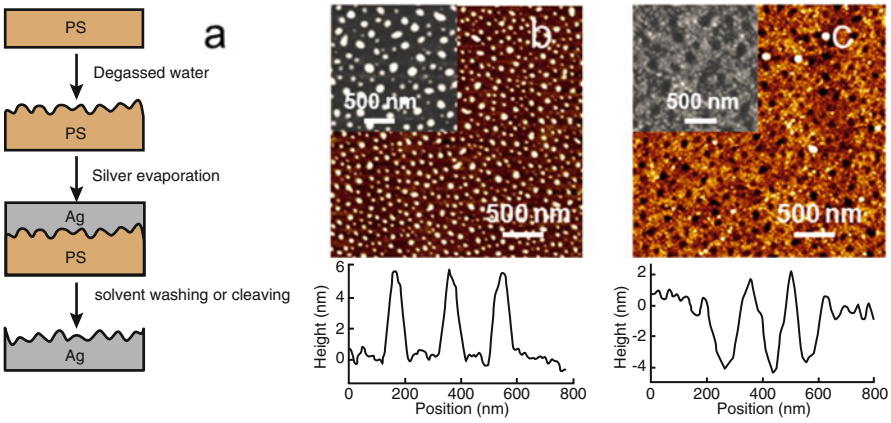

Fig. 11.10 The polymer-modified surfaces can also be used as a template to pattern metallic films as outlined in (**a**). Evaporating a 250 nm thick silver film on a structured PS film and removing the polymer film after gluing the stack onto a convenient substrate allow producing a metallic film of controlled surface structure with bumps (**b**) or holes (**c**). Adapted with permission from [21]. Copyright (2011) American Chemical Society

References

1. Parker, J.L., Claesson, P.M., Attard, P.: Bubbles, cavities, and the long-ranged attraction between hydrophobic surfaces. J. Phys. Chem. **98**, 8468–8480 (1994)
2. Zhang, X.H., Zhang, X., Sun, J., Zhang, Z., Li, G., Fang, H., Xiao, X., Zeng, X., Hu, J.: Detection of novel gaseous states at the highly oriented pyrolytic graphite-water interface. Langmuir **23**, 1778–1783 (2007)
3. Seddon, J.R.T., Bliznyuk, O., Kooij, E.S., Poelsema, B., Zandvliet, H.J.W., Lohse, D.: Dynamic dewetting through micropancake growth. Langmuir **26**, 9640–9644 (2010)
4. Attard, P.: The stability of nanobubbles. Eur. Phys. J. Spec. Top. 1–22 (2013). doi:10.1140/epjst/e2013-01817-0
5. Seddon, J.R.T., Lohse, D.: Nanobubbles and micropancakes: gaseous domains on immersed substrates. J. Phys. Condens. Matter **23**, 133001 (2011)
6. Zhang, X., Khan, A., Ducker, W.: A nanoscale gas state. Phys. Rev. Lett. **98**, 136101 (2007)
7. Martinez, J., Stroeve, P.: Transient behavior of the hydrophobic surface/water interface: from nanobubbles to organic layer. J. Phys. Chem. B **111**, 14069–14072 (2007)
8. Karpitschka, S., Dietrich, E., Seddon, J.R.T., Zandvliet, H.J.W., Lohse, D., Riegler, H.: Nonintrusive optical visualization of surface nanobubbles. Phys. Rev. Lett. **109**, 066102 (2012)
9. Switkes, M., Ruberti, J.W.: Rapid cryofixation/freeze fracture for the study of nanobubbles at solid–liquid interfaces. Appl. Phys. Lett. **84**, 4759 (2004)
10. Seddon, J.R.T., Kooij, E.S., Poelsema, B., Zandvliet, H.J.W., Lohse, D.: Surface bubble nucleation stability. Phys. Rev. Lett. **106**, 056101 (2011)
11. Ducker, W.A.: Contact angle and stability of interfacial nanobubbles. Langmuir **25**, 8907–8910 (2009)
12. Brenner, M., Lohse, D.: Dynamic equilibrium mechanism for surface nanobubble stabilization. Phys. Rev. Lett. **101**, 214505 (2008)
13. Mazumder, M., Bhushan, B.: Propensity and geometrical distribution of surface nanobubbles: effect of electrolyte, roughness, ph, and substrate bias. Soft Matter **7**, 9184 (2011)
14. Onsager, L., Samaras, N.N.T.: The surface tension of Debye-Hückel electrolytes. J. Chem. Phys. **2**, 528 (1934)
15. Noah-Vanhoucke, J., Geissler, P.L.: On the fluctuations that drive small ions toward, and away from, interfaces between polar liquids and their vapors. Proc. Natl. Acad. Sci. U. S. A **106**, 15125–15130 (2009)
16. Kudin, K.N., Car, R.: Why are water-hydrophobic interfaces charged? J. Am. Chem. Soc. **130**, 3915–3919 (2008)
17. Jungwirth, P., Tobias, D.J.: Molecular structure of salt solutions: a new view of the interface with implications for heterogeneous atmospheric chemistry. J. Phys. Chem. B **105**, 10468–10472 (2001)
18. Gray-Weale, A., Beattie, J.K.: An explanation for the charge on water's surface. Phys. Chem. Chem. Phys. **11**, 10994–11005 (2009)
19. Zangi, R., Engberts, J.B.F.N.: Physisorption of hydroxide ions from aqueous solution to a hydrophobic surface. J. Am. Chem. Soc. **127**, 2272–2276 (2005)
20. Hunter, R.J.: Foundations of colloid science, 2nd edn. Oxford University Press, Oxford (2001)
21. Siretanu, I., Chapel, J.P., Drummond, C.: Water-ions induced nanostructuration of hydrophobic polymer surfaces. ACS Nano **5**, 2939–2947 (2011)
22. Pashley, R.M.: Effect of degassing on the formation and stability of surfactant-free emulsions and fine teflon dispersions. J. Phys. Chem. B **107**, 1714–1720 (2003)
23. Beattie, J.K., Djerdjev, A.M.: The pristine oil/water interface: surfactant-free hydroxide-charged emulsions. Angew. Chem. Int. Ed. Engl. **43**, 3568–3571 (2004)
24. Maeda, N., Rosenberg, K.J., Israelachvili, J.N., Pashley, R.M.: Further studies on the effect of degassing on the dispersion and stability of surfactant-free emulsions. Langmuir **20**, 3129–3137 (2004)

25. Snoswell, D.R.E., Duan, J., Fornasiero, D., Ralston, J.: Colloid stability and the influence of dissolved gas. J. Phys. Chem. B **107**, 2986–2994 (2003)
26. Meyer, E.E., Lin, Q., Israelachvili, J.N.: Effects of dissolved gas on the hydrophobic attraction between surfactant-coated surfaces. Langmuir **21**, 256–259 (2005)
27. Pashley, R.M., Rzechowicz, M., Pashley, L.R., Francis, M.J.: De-gassed water is a better cleaning agent. J. Phys. Chem. B **109**, 1231–1238 (2005)
28. Dai, Z., Fornasiero, D., Ralston, J.: Influence of dissolved gas on bubble-particle heterocoagulation. J. Chem. Soc. Faraday Trans. **94**, 1983–1987 (1998)
29. Cottin-Bizonne, C., Cross, B., Steinberger, A., Charlaix, E.: Boundary slip on smooth hydrophobic surfaces: intrinsic effects and possible artifacts. Phys. Rev. Lett. **94**, 056102 (2005)
30. Wang, Y., Bhushan, B., Zhao, X.: Nanoindents produced by nanobubbles on ultrathin polystyrene films in water. Nanotechnology **20**, 045301 (2009)
31. Janda, P., Frank, O., Bastl, Z., Klementová, M., Tarábková, H., Kavan, L.: Nanobubble-assisted formation of carbon nanostructures on basal plane highly ordered pyrolytic graphite exposed to aqueous media. Nanotechnology **21**, 095707 (2010)
32. Tarábková, H., Janda, P.: Nanobubble assisted nanopatterning utilized for ex situ identification of surface nanobubbles. J. Phys. Condens. Matter **25**, 184001 (2013)
33. Fakhraai, Z., Forrest, J.A.: Measuring the surface dynamics of glassy polymers. Science **319**, 600–604 (2008)
34. Manciu, M., Ruckenstein, E.: On the interactions of ions with the air/water interface. Langmuir **21**, 11312–11319 (2005)
35. Levin, Y.: Polarizable ions at interfaces. Phys. Rev. Lett. **102**, 147803 (2009)
36. Parsegian, V.A.: Ion-membrane interactions as structural forces. Ann. N. Y. Acad. Sci. **264**, 161–174 (1975)
37. Horinek, D., Herz, A., Vrbka, L., Sedlmeier, F., Mamatkulov, S.I., Netz, R.R.: Specific ion adsorption at the air/water interface: the role of hydrophobic solvation. Chem. Phys. Lett. **479**, 173–183 (2009)
38. Shanahan, M.E., Carré, A.: Spreading and dynamics of liquid drops involving nanometric deformations on soft substrates. Colloids. Surf. A. Physicochem. Eng. Asp. **206**, 115–123 (2002)
39. Zimmermann, R., Freudenberg, U., Schweiß, R., Küttner, D., Werner, C.: Hydroxide and hydronium ion adsorption – a survey. Curr. Opin. Colloid Interface Sci. **15**, 196–202 (2010)
40. Jungwirth, P., Tobias, D.J.: Specific ion effects at the air/water interface. Chem. Rev. **106**, 1259–1281 (2006)
41. Siretanu, I., Chapel, J.-P., Bastos-González, D., Drummond, C.: Ions-induced nanostructuration: effect of specific ionic adsorption on hydrophobic polymer surfaces. J. Phys. Chem. B **117**, 6814–6822 (2013)
42. Buck, E., Petersen, K., Hund, M., Krausch, G., Johannsmann, D.: Decay kinetics of nanoscale corrugation gratings on polymer surface: evidence for polymer flow below the glass temperature. Macromolecules **37**, 8647–8652 (2004)
43. Siretanu, I., Chapel, J.P., Drummond, C.: Substrate remote control of polymer film surface mobility. Macromolecules **45**, 1001–1005 (2012)